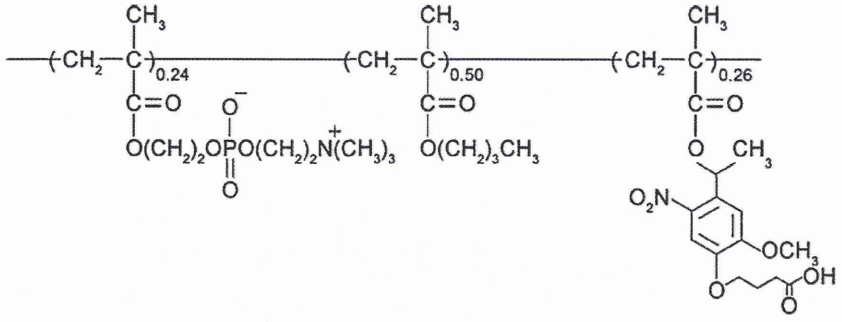

Fig. 1. Chemical structure of photoreactive phospholipid polymer (PMB-PL).

using a phase-contrast microscope. UV light (360 nm, 80 mW/cm^2) was administered to the PMB-PL surface for 60 s. Detached cells following UV-irradiation were recovered and calculated for cell density using a hemocytometer. After irradiation, the culture dish plate was washed with PBS, and the remaining cells were detached using the abovementioned trypsin method. Detached cells were counted and cell counts were converted to cell density per unit area (cells/cm^2).

3. Result and discussion

A photoreactive phospholipid polymer (PMB-PL) was synthesized with MPC, BMA, and PL monomer via the conventional radical polymerization technique. The chemical structure of PMB-PL is shown in Fig. 1. The monomer unit composition of the PMB-PL polymer was calculated by ^{1}H NMR measurement as MPC/BMA/PL = 0.24/0.50/0.26. The PMB-PL was soluble in organic solvents such as alcohol, dimethylsulfoxide, and dioxane. The molecular weight was $M_w = 1.43 \times 10^4$ and average molecular weight was calculated by GPC measurement based on poly(ethylene oxide) (PEO) standards to be M_w/M_n was 1.31.

To evaluate the photochemical activity, PMB-PL was dissolved in ethanol and its spectral change in response to UV light irradiation ($\lambda > 200$ nm) was examined. Before UV irradiation, the solution showed absorption transitions at 300 nm and 348 nm typical for a 3,4-dimethoxy-6-nitrophenyl group [30]. After UV irradiation, the spectrum showed a dose-dependent decrease at the 348-nm transition while two new adsorption transitions appeared at 265 nm and 375 nm. These new adsorption peaks belong to the 4-(4-acetyl-2-methoxy-5-nitrophenoxy)butanoic acid photoproduct, which indicates that the PMB-PL in bulk solution undergoes a photochemical reaction that is characteristic of the 2-nitrobenzyl ester. The PMB-PL after photoirradiation can be soluble in methanol, ethanol, and dimethyl sulfoxide.

The surface of the quartz crystal glass was subjected to UV-ozone treatment, and the glass was immersed in a PMB-PL ethanol solution for several minutes. This process was repeated thrice. After UV irradiation ($\lambda > 200$ nm), the PMB-PL modified glass was washed with distilled water and the UV spectrum was measured. Before UV irradiation, the modified substrate surface showed a similar absorption spectrum between 250 and 400 nm (Fig. 2) as that of the PMB-PL in solution phase. After UV-irradiation, the transition intensity at 348 nm decreased similar to that of PMB-PL

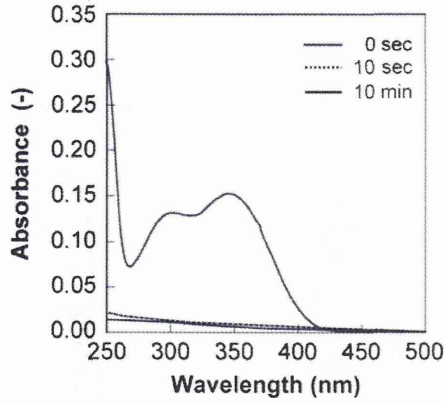

Fig. 2. Absorbance spectra of PMB-PL modified quartz glass surface, which were measured under varied UV-irradiation times.

in bulk solution. However, the transitions at 265 nm and 375 nm corresponding to the elimination of the 4-(4-acetyl-2-methoxy-5-nitrophenoxy)butanoic acid photoproduct by washing, were not observed. These results indicate that the PMB-PL retained its photochemical activity.

The changes in the surface features before and after UV-irradiation are summarized in Table 1. XPS analysis indicated that the PMB-PL modified surface had a phosphorus peak, a nitrogen peak, an oxygen peak, a silicon peak, and a strong carbon peak. After a 10 min UV-irradiation period, the *P/C* ratio on the PMB-PL modified surface increased and the N/C, O/C ratios decreased. These results support the notion that the ester groups on the PMB-PL surface are photocleaved under UV-light.

Ellipsometric measurement revealed that the thickness of the PMB-PL surfaces were 25 ± 7 nm under dry conditions. In addition, from atomic force microscopy (AFM, Nihon Veeco, Tokyo, Japan) observations, the root mean square roughness (RMS) of the PMB-PL surface was calculated as 0.826, which suggests a smooth surface obtained by spin coating (data not shown). The static wettability of the PMB-PL surface was estimated for the air-in-water and water-in-air systems (Table 1). During UV-irradiation of the air-in-water system, the water contact angle ($\beta = 180^\circ - \theta$) was changed from 48° to 34°, which suggests a more hydrophilic surface was observed after 10 min of photolysis. This result indicates that the

Table 1
Changes in PMB-PL surface features before and after UV-irradiation.

PMB-PL surface	Ellipsometric thickness (nm)	Contact angle (°)		*P/C* (-)	ζ-potential (mV)
		Water-in-air	Air-in-water		
Before irradiation	25 ± 7	88	48	0.088	−44.3
After irradiation	25 ± 7	111	34	0.145	−2.1

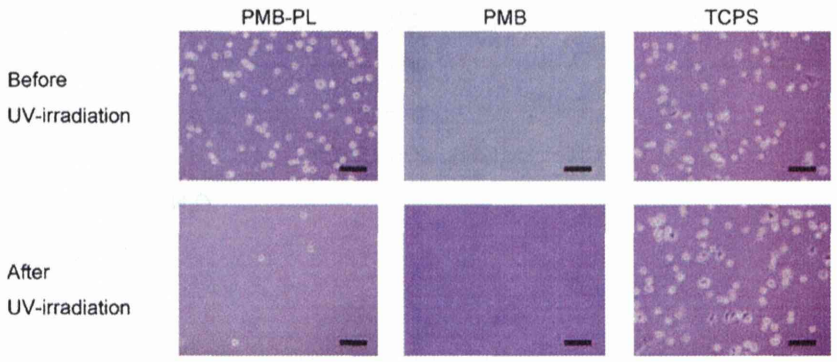

Fig. 3. Phase contrast microscope images (scale = 100 μm) displaying HeLa cells on PMB-PL, PMB, and TCPS surfaces. The upper images were taken before UV irradiation and the lower images were taken following irradiation.

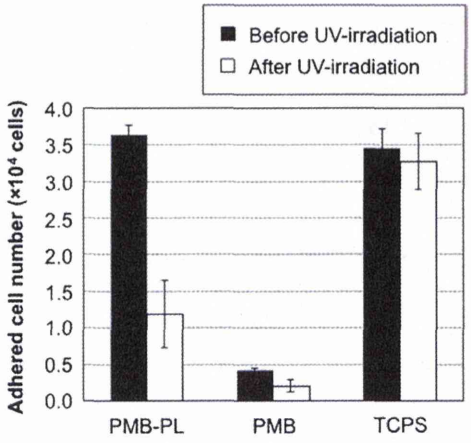

Fig. 4. Adhered cell number on PMB-PL, PMB, and TCPS surfaces shown on left side and detached cell number after UV-irradiation for respective surfaces on right.

surface was mostly converted to the hydrophilic phosphorylcholine (PC) groups, which results from removing the photocleavable PL groups from the substrate. In contrast, for the water-in-air system, the surface static contact angle changed from 88° to 101° which indicates a more hydrophobic surface was obtained after 10 min of light exposure. These results occur because under dry conditions, the PC groups migrate into the inner area and, consequently, leave the hydrophobic butyl methacrylate (BMA) units covered at the uppermost substrate surface. This indicates that surface chemical composition and surface wettability can be controlled using an external UV-light stimulus.

The surface ζ-potential of the PMB-PL surface was −44.3 mV, which is strongly negative. During UV irradiation, the surface ζ-potential changed to −2.1 mV (Table 1), which is a result of an increase in the composition of the MPC unit in the PMB-PL. This increase is attributed to an increase in PL unit photocleavage. It is well reported that the zwitterionic PC groups in PMB-PL surface form an inner salt and thus the electrostatic effects diminish [31–34]. When the composition of the MPC units increased, the surface ζ-potential of the PMB-PL surface was close to zero. This result was in agreement with the results of the static contact angle measurement. From the contact angle measurement and surface ζ-potential measurement, it is concluded that the negatively charged hydrophilic PMB-PL surface is changed to a neutrally charged more hydrophilic surface during UV-photolysis.

Cell attachment and detachment on the PMB-PL surface with UV-irradiation were also examined. In this experiment we used the photoreactive PMB-PL surface, a PMB surface that did not contain the photocleavable PL moiety, and the conventional tissue culture treated polystyrene (TCPS). Fig. 3 shows the phase-contrast

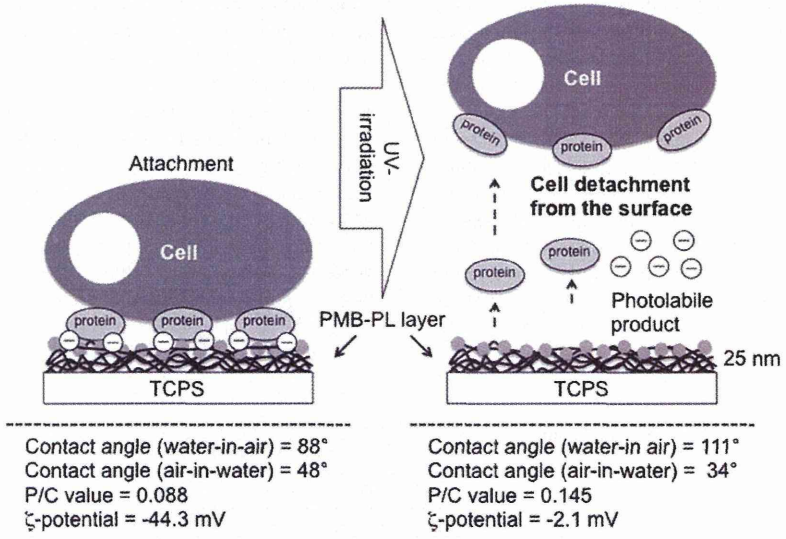

Fig. 5. Schematic of cell attachment/detachment at PMB-PL surface based on alteration of surface properties following UV-irradiation.

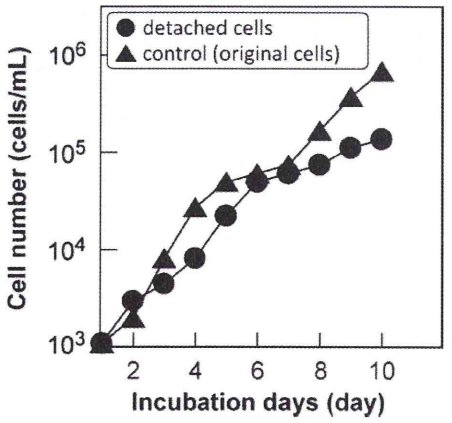

Fig. 6. Cell number dependency on incubation time. The cells were detached from the PMB-PL surface using UV-irradiation.

microscope images of the HeLa cells before and after UV irradiation, and Fig. 4 shows the cell density on each surface before and after irradiation. From the calculations, it was concluded that more than 90% of the seeded cells were attached onto the PMB-PL surface, and 67% of attached cells were detached by photo-irradiation. In the case of the PMB-only surface and the TCPS, less than 5% of the seeded cells were detached following UV-irradiation. This result indicates that UV-exposure induces detachment of attached cells. The proposed mechanism by which this occurs is as follows: the cells are initially bound to the cell-adhesive proteins via the photocleavable PL unit; the PL units are cleaved following the photochemical reaction and the non-biofouling surface of phosphorylcholine groups remain intact at the substrate surface. In generally, the cells were adhered through the adsorbed protein on the substrate. In this study, the cell adhesive experiment was performed in the serum containing medium. Under the condition, it is considered the protein adsorption from the medium is considered to have occurred prior to the cell adhesion. Fig. 5 shows a schematic of cell attachment/detachment processes at the PMB-PL surface based on alteration of the surface properties using UV-irradiation. These results demonstrate the selective detachment of cells at the PMB-PL modified surface, which was related to the photocleavage of the PL unit using UV-irradiation.

Cell attachment and detachment behavior at the PMB-PL surface was also observed using fibroblast cells, L929 (data not shown). These results indicate that the mechanism of cell attachment and detachment on the PMB-PL surface was a consequence of the change in surface properties due to the photocleavage of the PL unit.

We also examined cell proliferation activity after the photoinduced detachment. The detached cells were cultured under usual culture conditions. Fig. 6 shows the cell proliferation of the detached HeLa cells from the PMB-PL surface. The detached cells from PMB-PL after photoirradiation proliferated at the same rate as the normal (original) cells cultured under usual conditions. The PMB-PL detached cells maintained their physiological properties, indicating that the UV-irradiation process did not affect the cell viability, and the PMB-PL surface non-invasively recovered the attached cells.

4. Conclusions

A photoreactive and cytocompatible phospholipid polymer, PMB-PL, was prepared and its surface properties were characterized. The substrate was modified to an extent that it allowed for the study of the photocleaving properties at the surface. Before UV-irradiation, the PMB-PL surface was negatively charged and relatively hydrophobic, which provided protein adsorption and cell adhesion. After irradiation, the surface was neutrally charged and hydrophilic because of the MPC unit. The PMB-PL surface induced cell attachment, and was externally stimulated using UV-light allowing cell detachment from the surface, while maintaining cell viability. Furthermore, the PL monomer unit has a carboxylic group in the side chain, which provides a site for conjugation by desired biomolecules at the PMB-PL surface. The PMB-PL surface is a valuable tool to investigate the bioactivity of conjugated biomolecules, and affords a selective mechanism by which specific cells can be recovered from the surface using UV-light. Selective cell collection and analysis of the cell function at the surface will be reported elsewhere. The development of the PMB-PL surface and the selective detachment of the cells using UV-irradiation has been shown to be a promising and valuable technique for applications in cell analysis and more specifically single-cell analysis.

Acknowledgments

The authors would like to express gratitude to Dr. Hisashi Sugiyama at Hitachi High-Technologies and Mr. Satoshi Ozawa at Central Research Laboratory, Hitachi Co., Ltd. for their valuable discussions.

Appendix A. Supplementary data

Supplementary data associated with this article can be found, in the online version, at doi:10.1016/j.colsurfb.2011.08.029.

References

[1] A.S. Hoffman, Macromol. Symp. 98 (1995) 645.
[2] A.S. Hoffman, Artif. Org. 19 (1995) 458.
[3] P.M. Mendes, Chem. Soc. Rev. 37 (2008) 2512.
[4] N. Nath, A. Chilkoti, Adv. Mater. 14 (2002) 1243.
[5] M.A.C. Stuart, W.T.S. Huck, J. Genzer, M. Müller, C. Ober, M. Stamm, G.B. Sukhorukov, I. Szleifer, V.V. Tsukruk, M. Urban, F. Winnik, S. Zauscher, I. Luzinov, S. Minko, Nat. Mater. 9 (2010) 101.
[6] H. Kaji, M. Kanada, D. Oyamatsu, T. Matsue, M. Nishizawa, Langmuir 20 (2004) 16.
[7] X. Jiang, R. Ferrigno, M. Mrksich, G.M. Whitesides, J. Am. Chem. Soc. 125 (2003) 2366.
[8] W.S. Yeo, M.N. Yousaf, M. Mrksich, J. Am. Chem. Soc. 125 (2003) 14994.
[9] M.N. Yousaf, B.T. Houseman, M. Mrksich, Proc. Natl. Acad. Sci. U.S.A. 98 (2001) 5992.
[10] N. Yamada, T. Okano, H. Sakai, F. Karikusa, Y. Sawasaki, Y. Sakurai, Makromol. Chem. Rapid Commun. 11 (1990) 571.
[11] T. Okano, N. Yamada, H. Sakai, Y. Sakurai, J. Biomed. Mater. Res. 27 (1993) 1243.
[12] T. Okano, N. Yamada, M. Okuhara, H. Sakai, Y. Sakurai, Biomaterials 16 (1995) 297.
[13] M.D. Wilson, G.M. Whitesides, J. Am. Chem. Soc. 110 (1988) 8718.
[14] M. Motornov, R. Sheparovych, R. Lupitskyy, E. MacWilliams, O. Hoy, Adv. Funct. Mater. 17 (2007) 2307.
[15] N. Ayres, C.D. Cyrus, W.J. Brittain, Langmuir 23 (2007) 3744.
[16] N. Negishi, T. Iida, K. Ishihara, I. Shinohara, Makromol. Chem. Rapid Commun. 2 (1981) 617.
[17] K. Ishihara, S. Kato, I. Shinohara, J. Appl. Polym. Sci. 27 (1982) 4273.
[18] K. Ishihara, M. Kim, I. Shinohara, T. Okano, K. Kataoka, Y. Sakurai, J. Appl. Polym. Sci. 28 (1983) 1321.
[19] J. Nakanishi, Y. Kikuchi, T. Takarada, H. Nakayama, K. Yamaguchi, M. Maeda, J. Am. Chem. Soc. 126 (2004) 16314.
[20] K. Ishihara, H. Nomura, T. Mihara, K. Kurita, Y. Iwasaki, N. Nakabayashi, J. Biomed. Mater. Res. 39 (1998) 323.
[21] K. Ishihara, E. Ishikawa, Y. Iwasaki, N. Nakabayashi, J. Biomater. Sci. Polym. Ed. 10 (1999) 1047.
[22] T. Konno, K. Akita, K. Kurita, Y. Ito, J. Biosci. Bioeng. 100 (2005) 88.
[23] T. Konno, K. Ishihara, Biomaterials 28 (2007) 1770.
[24] S. Sawada, S. Sakaki, Y. Iwasaki, N. Nakabayashi, K. Ishihara, J. Biomed. Mater. Res. 64A (2003) 411.
[25] K. Jang, K. Sato, K. Mawatari, T. Konno, K. Ishihara, T. Kitamori, Biomaterials 30 (2009) 1413.
[26] T. Konno, H. Hasuda, K. Ishihara, Y. Ito, Biomaterials 26 (2005) 1381.
[27] T. Konno, N. Kawazoe, G. Chen, Y. Ito, J. Biosci. Bioeng. 102 (2006) 304.

[28] K. Jang, Y. Xu, Y. Tanaka, K. Sato, K. Mawatari, T. Konno, K. Ishihara, T. Kitamori, Biomicrofluidics 4 (2010) 032208.
[29] S.P. Adams, R.Y. Tsien, Annu. Rev. Physiol. 55 (1993) 755.
[30] K. Ishihara, T. Ueda, N. Nakabayashi, Polym. J. 22 (1990) 355.
[31] J. Ottl, D. Gabriel, G. Marriott, Bioconjug. Chem. 9 (1998) 143.
[32] T. Ueda, K. Ishihara, N. Nakabayashi, J. Biomed. Mater. Res. 29 (1995) 381.
[33] Y. Inoue, J. Watanabe, K. Ishihara, J. Colloid Interface Sci. 274 (2004) 465.
[34] T. Konno, K. Kurita, Y. Iwasaki, N. Nakabayashi, K. Ishihara, Biomaterials 22 (2001) 1883.

Colloids and Surfaces B: Biointerfaces 97 (2012) 70–76

Contents lists available at SciVerse ScienceDirect

Colloids and Surfaces B: Biointerfaces

journal homepage: www.elsevier.com/locate/colsurfb

Simple surface treatment using amphiphilic phospholipid polymers to obtain wetting and lubricity on polydimethylsiloxane-based substrates

Kyoko Fukazawa [a], Kazuhiko Ishihara [a,b,*]

[a] Department of Materials Engineering, School of Engineering, The University of Tokyo, 7-3-1, Hongo, Bunkyo-ku, Tokyo 113-8656, Japan
[b] Department of Bioengineering, School of Engineering, The University of Tokyo, 7-3-1, Hongo, Bunkyo-ku, Tokyo 113-8656, Japan

ARTICLE INFO

Article history:
Received 13 February 2012
Received in revised form 3 April 2012
Accepted 4 April 2012
Available online 13 April 2012

Keywords:
Polydimethylsiloxane
Surface treatment
Phospholipid polymer
Wettability
Lubrication property

ABSTRACT

Simple surface treatment of polydimethylsiloxane (PDMS) substrates was performed using an aqueous-ethanolic solution of amphiphilic phospholipid polymers to reduce the hydrophobic and high friction characteristics of PDMS. The phospholipid polymers, poly(2-methacryloyloxyethyl phosphorylcholine (MPC)-*co*-2-ethylhexyl methacrylate (EHMA)-*co*-2-(*N*,*N*-dimethylamino)ethyl methacrylate) (PMED) and poly(MPC-*co*-EHMA) (PMEH) were synthesized, and the effects of the electric charge of the polymer chain on the stability of the attachment to the PDMS surface was investigated. The polymers were dissolved in a mixed solvent of ethanol and water, and the PDMS samples were treated by a simple dipping method using the polymer solution. Pure ethanol as the solvent was ineffective for the attachment of the polymers to the PDMS surface. It was considered that the hydrophobic interactions and electrostatic attraction forces between the polymer chains and the PDMS surface were too weak for efficient interaction in this solvent. On the other hand, the surface wettability and lubricity of PDMS could be improved by treatment with an aqueous-ethanolic solution of PMED. The static contact angle was decreased from 90° to 20° by this treatment, and the dynamic friction coefficient against a Co–Cr ball was decreased by nearly 80% compared with that of the untreated PDMS. The hydrophobic interactions and electrostatic attraction forces generated by PMED were both essential for the stable adsorption of the polymer layer on PDMS. Furthermore, the solubilized state of the polymers affected the adsorption of the polymer. We concluded that the surface of PDMS could be stably modified using aqueous-ethanolic solutions of PMED without the need for pretreatments.

1. Introduction

Polydimethylsiloxane (PDMS) is one of the most frequently used materials for medical devices such as catheters, endoscopes, dentures, finger joints, and contact lenses owing to its attractive properties such as high flexibility, processability, good mechanical properties, high gas permeability and optical transparency [1–3]. However, the native hydrophobicity, high friction, and biofouling tendency of PDMS limit its applications in biological environments. A number of attempts have been made to decrease the hydrophobicity and suppress the nonspecific adsorptions of PDMS by means of surface modification [4–10]. Oxygen plasma treatment is one such technique that has been widely used for modification of the surface hydrophobicity. However, the hydrophilicity conferred by this process is temporary and the surface recovers its hydrophobic property within a short time [11–13]. In addition, the oxygen plasma cannot be applied to the inner surfaces of thin tubes such as catheters and endoscopes from the viewpoint of mean free path. Surface modification of PDMS using biocompatible polymers represents an alternative technique for changing the surface properties. The use of 2-methacryloyloxyethyl phosphorylcholine (MPC) polymers has proved to be particularly promising for improving the biocompatibility of the surface of biomedical devices [14–17]. MPC polymers contain extremely hydrophilic phosphorylcholine groups in their side chain, and surfaces covered with MPC polymers exhibit good wettability, low friction, and resistance to protein adsorption [18–21]. In fact, MPC polymers have been applied to several medical devices such as artificial hip joints [22,23], implantable blood pumps, cardiovascular stents, and contact lenses. Surface modification of PDMS with MPC has been undertaken in various studies by means of either chemical reaction or physical adsorption. Goda et al. introduced poly(MPC) (PMPC) chains onto the PDMS surface by photoinduced graft polymerization [24,25]. Iwasaki et al. modified the PDMS surface by using well-defined ABA-type triblock copolymers composed of PMPC segments (A) and a central PDMS segment (B) with anchoring vinyl groups. The hydrosilylated PDMS surface reacted with vinyl groups of the B

* Corresponding author at: Department of Materials Engineering, School of Engineering, The University of Tokyo, 7-3-1, Hongo, Bunkyo-ku, Tokyo 113-8656, Japan. Tel.: +81 3 5841 7124; fax: +81 3 5841 8647.
E-mail address: ishihara@mpc.t.u-tokyo.ac.jp (K. Ishihara).

0927-7765/$ – see front matter © 2012 Elsevier B.V. All rights reserved.
http://dx.doi.org/10.1016/j.colsurfb.2012.04.008

blocks [26]. This method successfully improved the surface wettability and lubrication and decreased the biofouling tendency of PDMS. Although the modification of the PDMS surface with MPC via a chemical reaction is a powerful tool for enhancing the properties of PDMS, the process is complex and it is difficult to modify intricately shaped devices after fabrication. More practical methods have been reported by Sibarani et al., who modified the PDMS surface by a simple treatment method [27], and Seo et al., who modified the PDMS surface by swelling–deswelling methods using ABA-type block copolymers composed of PMPC (A) and PDMS (B) segments [28]. The relative simplicity of these processes renders them more applicable than grafting polymerization and chemical reaction processes. However, the disadvantage of these methods is that low-polarity solvents such as chloroform are used for the surface treatment process because of the low surface energy of PDMS. These solvents induce swelling of PDMS, and consequently, this method is unsuitable for tailor-made devices with dimension-specific designs. On the other hand, the adsorption of poly(ethylene oxide)-*block*-poly(propylene oxide)-*block*-poly(ethylene oxide) and poly(L-lysine)-*graft*-poly(ethylene glycol) (PLL-*g*-PEG) on hydrophobic surfaces in aqueous environments has been reported [29–31]. Lee et al. investigated the adsorption behavior of PLL-*g*-PEG on the PDMS surface by changing the molecular weight of the copolymer and varying the solvent parameters such as pH and salt concentration. They suggested that the large number of hydrophobic groups in the copolymer and the extended conformation of the polymer in aqueous solution are associated with the ease of adsorption of the polymer [31]. For surface modification of biomedical devices, stability of the adsorbed polymer layer under aqueous conditions is essential. In general, proteins can be readily adsorbed from an aqueous medium onto various surfaces. Surface adsorption is normally irreversible owing to conformational changes of the proteins on the surface. Although surface adsorption of protein is a complex process, hydrophobic interaction and electrostatic forces generated at the interface are some of the dominant forces [32]. When proteins approach a surface, the water molecules between surrounding proteins and the surface are removed by an entropic effect. This phenomenon induces a conformational change in the proteins, and the proteins are irreversibly adsorbed on the surface by hydrophobic interaction and electrostatic interaction. We hypothesized that a molecular design similar to the protein structure, with hydrophobic portions and electric charges, should be suitable for the surface treatment of PDMS. PDMS is an elastic material, its surface is hydrophobic, and its surface ζ potential is −44.1 mV [27]. Therefore, we chose 2-ethylhexyl methacrylate (EHMA) and 2-(*N*,*N*-dimethylamino)ethyl methacrylate (DMAEMA) as monomer units of the MPC polymer, with the expectation of hydrophobic interactions and electrostatic attraction forces. The objective of this study was to modify the PDMS surface with the MPC polymer by simple treatment from aqueous solution, thereby negating the swelling effects of low-polarity solvents on PDMS. The influence of the electric charge of the polymer chain and the polymer conformation in aqueous solution on the modification of the PDMS surface is investigated herein by varying the ratio of water and ethanol in the mixture used as the solvent.

2. Experimental

2.1. Materials

MPC was synthesized according to a previously reported method [33]. EHMA, DMAEMA and sodium 1-anilino-8-naphtalene sulfonate (ANS-Na) were purchased from Tokyo Kasei Kogyo (Tokyo, Japan). Liquid PDMS (Silpot 184®) and its curing agent were purchased from Toray-Dow Corning Asia Co. The other reagents and solvents were commercially available in extra-pure grade and used without further purification.

2.2. Synthesis of positively charged amphiphilic polymer

Poly(MPC-*co*-EHMA-*co*-DMAEMA) (PMED) and poly(MPC-*co*-EHMA) (PMEH) were synthesized by a conventional radical polymerization method in ethanol using 2,2′-azobisisobutyronitrile (AIBN) as the radical initiator. The polymerization was carried out at 60 °C. The formed polymer was purified by pouring the reaction mixture into an excess volume of ether/chloroform (8/2, v/v) for precipitation. Furthermore, unreacted MPC was removed by crushing the precipitated polymer and washing with water for 2.0 h. The polymer was collected by filtration and lyophilized. The chemical structure of the polymer was confirmed by ^{1}H NMR in CD_3CD_2OD, the molecular weight of the polymer was evaluated by gel permeation chromatography (GPC, Jasco, Tokyo, Japan) using hexafluoroisopropanol (HFIP) as the eluent, and the retention time was compared with that of the poly(methyl methacrylate) standard. The chemical structure of PMED and PMEH is shown in Fig. 1.

2.3. Fluorescence measurement using ANS-Na

The polarity of the PMED and PMEH solutions prepared in a mixed solvent with various ratios of ethanol and water was evaluated by fluorescence measurements using ANS-Na as a probe. The polymers were first completely dissolved in ethanol, and water was then added in a prescribed ratio. Subsequently, ethanolic ANS solution was added to each sample and the mixture kept in a dark place. The final polymer concentration was 1.0 wt% and the ANS-Na concentration was 1.0×10^{-5} M. The internal polarity of the polymer aggregate was estimated using the maximum wavelength from the fluorescence of ANS-Na (λ_{ex} = 350 nm, measurement range = 420–650 nm).

2.4. Preparation of PDMS

The precursor of PDMS and curing agent were mixed in a 10:1 (v/v) ratio. The mixtures were evenly spread on a dish and were placed under vacuum to remove air bubbles. The curing reaction was performed at 60 °C for 4.0 h.

2.5. Treatment process

PMED and PMEH were dissolved in ethanol and water was added in a given ratio. Ethanolic polymer (PMED and PMEH) solutions containing water at ratios of 0, 20, 50, and 80 v/v% were prepared and are hereafter referred to as PMED-0, 20, 50, and 80 and PMEH-0, 20, 50, and 80, respectively. The final polymer concentration was adjusted to 1.0 wt%. All PDMS substrates were washed with ethanol prior to the treatment process. The plates were dipped 5 times for a few seconds into the PMED solution and then dried in air. This process was repeated twice and the plates were then completely dried under vacuum.

2.6. Surface characterization

The hydrophilicity of the PMED- and PMEH-treated PDMS surfaces was evaluated by measurement of the air and water contact angles using a static contact angle goniometer (CA-W; Kyowa Interface Science Co., Tokyo, Japan). Water contact angles (θ_{water}) were measured under dry conditions and the air contact angles (θ_{air}) were measured in water. The PDMS substrate was cut to fit dimensions of 10 mm × 40 mm × 1.0 mm and 10 mm × 20 mm × 0.70 mm for the respective air and water contact angle measurements.

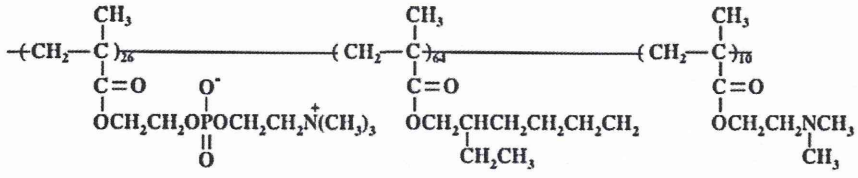

PMED Mw: 2.3 x 10^5

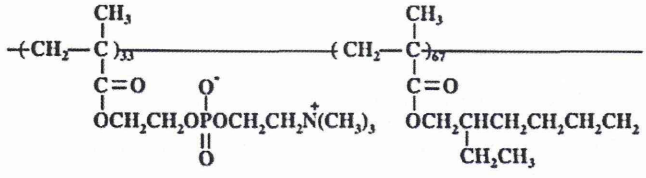

PMEH Mw: 1.2 x 10^5

Fig. 1. Chemical structure of MPC polymers.

The polymer-treated samples were immersed in water for 1 h and were dried under vacuum before contact angle measurements. In the measurement of θ_{water} under dry conditions, water droplets were brought into contact with the modified PDMS surface and θ_{water} was measured within 10 s using photographic images. θ_{air} was measured in water by attaching the samples to a sample holder, which was then transferred into a glass holder filled with purified water. After 5 min, air bubbles were introduced underneath each sample through U-shaped needles and the contact angles were measured using photographic images. Data were collected at 10 positions for each sample. The stability of the polymer layer was evaluated by immersing the samples in water for 1.0, 24, 72, 120, and 168 h. The surface elemental composition was analyzed using X-ray photoelectron spectroscopy (XPS; AXIS-His165 Kratos/Shimadzu, Kyoto, Japan). The photoelectron take-off angle was fixed at 90°. All of the binding energies were referenced to the C_{1s} peak at 285.0 eV and the corresponding peak areas were used to calculate the respective elemental compositions.

2.7. Friction test

The coefficients of dynamic friction between a Co–Cr ball and the surface of the polymer-treated PDMS samples were measured using a surface property tester (Heidon Type32, Shinto Science Co., Tokyo, Japan). The PDMS substrates were prepared in the box (65 mm × 35 mm × 3.0 mm) and were affixed to the stage. The friction tests were performed in purified water at room temperature with load of 0.98 N, for a maximum of 1.0×10^3 cycles.

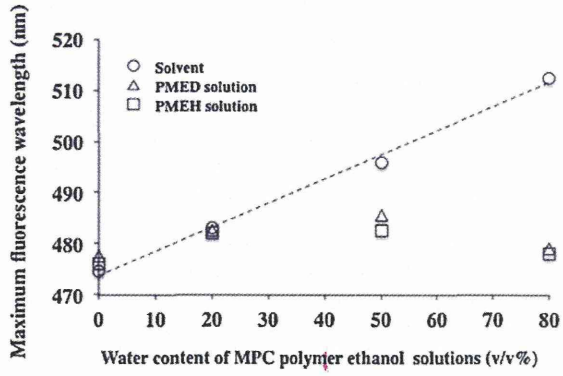

Fig. 2. Peak shifts of ANS-Na fluorescence in MPC polymer solutions.

The scan scale was 20 mm, and the scan speed was 40 mm/s. Three replicate measurements were performed for each sample, and the average values were regarded as the coefficients of dynamic friction.

3. Results and discussion

3.1. Characterization of the solubilized state of PMED in ethanol/water mixture

PMED and PMEH are both soluble in ethanol and do not dissolve in water. In addition, both polymers were soluble in ethanol/water mixtures. The polymer solution was transparent in water con-

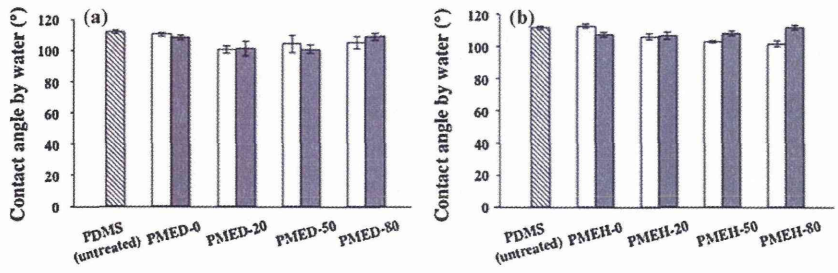

Fig. 3. The contact angles by water on the PDMS surface measured under dry conditions, before and after treatment with PMED (a) and PMEH (b) solution. Open column: just after treatment with the polymer solution. Closed column: after 1.0 h immersion in water.

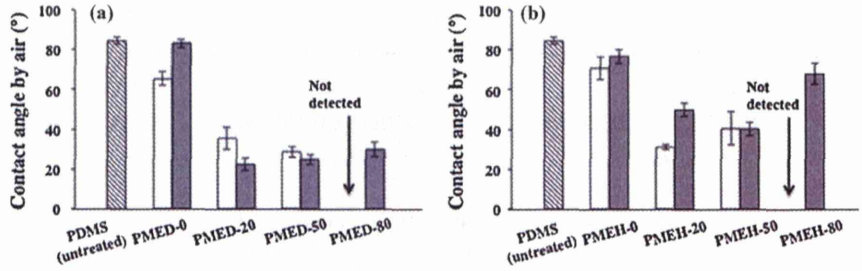

Fig. 4. The contact angles by air on the PDMS surface measured in aqueous solution, before and after coating with PMED (a) and PMEH (b) solution. Open column: just after coating. Closed column: after 1.0 h immersion in water.

tent ranges from 0 v/v% to 80 v/v%. Therefore, the conformation of the polymer changes in ethanol/water mixtures. The solubilized state of PMED and PMEH was evaluated after dissolution in ethanol/water mixtures of various ratios, using ANS-Na as a fluorescence probe. ANS-Na is sensitive to solvent polarity; the fluorescence quantum yield of ANS-Na is enhanced in hydrophobic environments, with a concomitant blue shift of the emission maximum [34]. Fig. 2 shows the emission maximum of ANS-Na in the solvent, PMED solution and PMEH solution. The maximum wavelength of fluorescence (λ_{max}) of ANS-Na in the 80 v/v% aqueous ethanolic solvent was 505 nm. However, the peak was blue-shifted with decreasing content of water. The λ_{max} of ANS-Na was almost the same in both the PMED and PMEH solutions. In the purely ethanolic and 20 v/v% aqueous-ethanolic polymer solutions, the λ_{max} of ANS-Na was almost same as that in the solvent. On the other hand, in the 50 v/v% and 80 v/v% aqueous-ethanolic polymer solutions, the λ_{max} was considerably lower than that in the solvent. The ratio of hydrophilic to hydrophobic units is almost same in both PMED and PMEH. These results indicate that both of the polymers undergo aggregation with increasing water content by hydrophobic interactions. In the 80 v/v% aqueous-ethanolic polymer solution, the polarity of the inside of the polymer aggregate was almost the same as that of ethanol.

3.2. Surface characterization of modified PDMS

The effect of the polymer conformation on the modification of the PDMS surface was investigated after dissolving PMED and PMEH in solvents with different ratios of ethanol to water. Fig. 3 shows the values of contact angles by water (θ_{water}) on the PDMS surface before and after treatment with PMED (a) and PMEH (b). In all samples, high values were obtained for the water contact angles under dry conditions, which were the same as those of untreated PDMS, and the values were not changed after immersion in water for 1 h. The phosphorylcholine group of the MPC polymers is hydrophilic, however, the hydrophobic units of the polymer are enriched at the air interface to decrease the surface free energy [35]. Fig. 4 shows the values of contact angles by air (θ_{air}) on the PDMS surface before and after treatment with PMED (a) and PMEH (b). In contrast to θ_{water} under dry conditions, θ_{air} in water were drastically decreased on the PMED and PMEH-treated surfaces, relative to the untreated surface, with the exception of the surface treated with PMED-0 and PMEH-0 (i.e., purely ethanolic) solutions. θ_{air} could not be measured on the surfaces treated with PMED-80 and PMEH-80, because the air bubble did not attach to the surface. The hydrophilic phosphorylcholine group is exposed in aqueous environments to reduce the interfacial free energy, thus, these results indicate successful treatment of the PDMS surface with PMED-20, 50, and 80 and PMEH-20, 50, and 80. After immersion in water for 1.0 h, the surfaces treated with PMED-20, 50, and 80 maintained their hydrophilicity. However, the contact angles of the surfaces treated with PMEH-20, 50, and 80 were increased after immersion in water for 1.0 h. In particular, the θ_{air} value of the surface treated with PMEH-80 was increased from 0° to 70°. These results indicate that PMEH-20, 50, and 80 were attached to the PDMS surface via weak interactions, and the polymer layer could be easily removed from the PDMS surface during immersion in aqueous solution. The success of the surface treatment with PMED and PMEH was further evaluated by XPS measurement. In the case of the surfaces treated with PMED-20, 50, and 80 and PMEH-20, 50, and 80, ammonium nitrogen and phosphorous peaks were observed at 403 eV and 133 eV, respectively. These atoms were attributed to the MPC unit. On the other hand, there were no peaks in the nitrogen region and phosphorous region for the surfaces treated with PMED-0 and PMEH-0. The results of the XPS and θ_{air} measurements reveal that when ethanol was used as a solvent (in the absence of water), the PDMS surface treatment process was unsuccessful. Fig. 5 shows the relationship between θ_{air} on the PDMS surfaces treated with PMED and PMEH versus the atomic ratio of P/Si of the surface. Contact angle and XPS values after immersion in water for 1.0 h were used for this plot. The atomic ratio of P/Si corresponded to the surface density of the MPC unit; therefore, the density of the phosphorylcholine group could be evaluated on this basis. The contact angle decreased

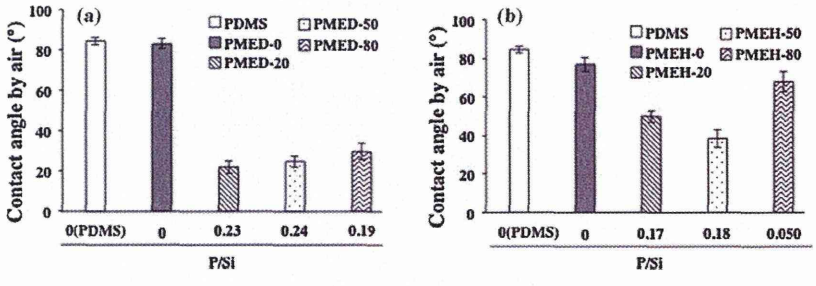

Fig. 5. Atomic ratio of P/Si on the PDMS surface coated with various MPC polymer solutions versus the air contact angles in an aqueous solution.

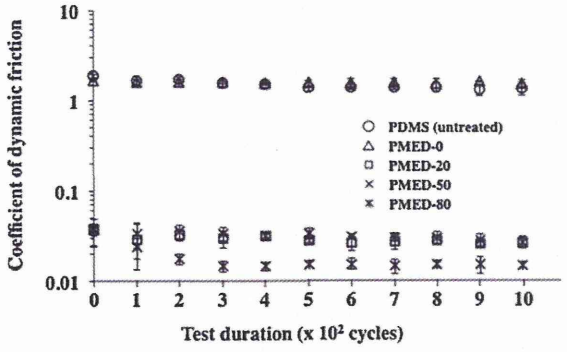

Fig. 6. Time course of the dynamic friction coefficient of the PDMS surface coated with PMED solution.

with an increase in the atomic ratio of P/Si, indicating that the wettability was conferred by the hydrophilic phosphorylcholine group.

3.3. Lubrication property

The lubricity of the surface is important for biomedical devices such as catheters, endoscopes, and artificial joints [19]. The dynamic friction coefficient was used as a parameter for characterizing the lubricity of the PDMS surface treated with PMED in water. Fig. 6 shows the time course of the dynamic friction coefficient between a Co–Cr ball and the surface of PMED-treated PDMS in water. The untreated PDMS surface and PMED-0 treated surface exhibited a very high dynamic friction coefficient of approximately 1.16, consistent with the unsuccessful treatment of the PDMS surface by PMED-0 indicated by the XPS and contact angle measurements. However, after treatment with PMED-20, 50, and 80, the dynamic friction coefficient was dramatically decreased to approximately 0.030, 0.030, and 0.015, respectively. This decrease is attributed to elimination of strong hydrophobic interactions by treatment with hydrophilic PMED. The hydrophilic state ensures the formation of an aqueous lubrication layer and reduces the friction force. The results of the lubrication tests corroborate with the results of the contact angle measurements. Furthermore, the low friction coefficient was maintained during 1.0×10^3 cycles at 0.98 N, demonstrating the stability of the PMED layer formed on the PDMS substrate during the treatment process.

3.4. Stability of MPC polymer on PDMS surface

The stability of the PMED and PMEH layers on the PDMS substrate in aqueous environments was further evaluated by XPS following surface treatment. Fig. 7 shows time course of the elemental ratio of P/Si for the PDMS surfaces treated with PMED (a) and PMEH (b). After immersion in water for 24 h, the atomic ratio of P/Si on the surface treated with PMED-50 and 80 decreased from 0.25 to 0.10. On the other hand, the atomic ratio of P/Si was maintained at 0.25 on the surface treated with PMED-20. All of the treated surfaces maintained an atomic ratio of P/Si of approximately 0.05 over the course of 168 h.

We have previously expounded the relationship between the amount of adsorbed fibrinogen and the surface P/Si ratio [36]. From that study, it is known that the fibrinogen adsorption capacity of the untreated PDMS surface is approximately 1.9 $\mu g/cm^2$. The amount of adsorbed fibrinogen was found to decrease with an increase in the atomic ratio of P/Si. In the case of a surface having an atomic ratio of P/Si of 0.035, the amount of fibrinogen adsorbed was significantly reduced to approximately 75% of that observed for the untreated PDMS. On this basis, it is predicted that the surface treated with PMED should exhibit good biofouling resistance after immersion in water for 168 h.

For the surfaces treated with PMEH-20 and 50, the atomic ratio of P/Si decreased from 0.25 to below 0.05 after immersion in water for 24 h, and for the surface treated with PMEH-80, the decrease was even more drastic, moving from approximately 0.15 to 0.05 over an immersion period of only 1.0 h. The P/Si ratio declined to almost 0 after immersion in water for 72 h for all of the treated surfaces. The pK_a of poly(DMAEMA) is about 8.0 [37,38]. In water (pH 5.6), more than 90% of the dimethyl amino groups are protonated. Therefore, PMED is positively charged and was more strongly adsorbed than PMEH; in particular, PMED-20 exhibited the highest stability among all the tested PMED types.

Fig. 8 shows an illustration of the relationship between the solubilized state of the polymer and the adsorption behavior of the polymer on the PDMS substrate. On the basis of the fluorescence measurements using ANS-Na, it was evident that neither PMED nor PMEH could form hydrophobic domains in the purely ethanolic and 20 v/v% aqueous-ethanolic solutions. On the other hand, hydrophobic domains were formed in the 50 v/v% and 80 v/v% aqueous-ethanolic solutions. In purely ethanolic solution, the hydrophobic interaction and electrostatic attraction forces were not operative between the polymer chains and the PDMS surface, therefore, there was no attachment of PMED and PMEH to the surface. In the 20 v/v% aqueous-ethanolic solutions of both polymers, the polymer chains were in the stretched conformation, and were adsorbed on the PDMS surface via hydrophobic interactions. However, the stability of the PMED layer on the surface was much higher than that of the PMEH layer. PMED possesses positive charges in the aqueous solution based on the DMAEMA units, whereas the PDMS surface is negatively charged. Therefore, the difference in the stability of the layers formed by PMED and PMEH suggests that PMED is adsorbed onto the PDMS surface not only by hydrophobic interactions but also by electrostatic attraction forces. In 50 v/v% and 80 v/v% aqueous-ethanolic solutions, PMED and PMEH could form aggregates, with hydrophobic interaction operating as the driving force for aggregation of the hydrophobic units. Because the hydrophobic domain was formed inside the polymer aggregate

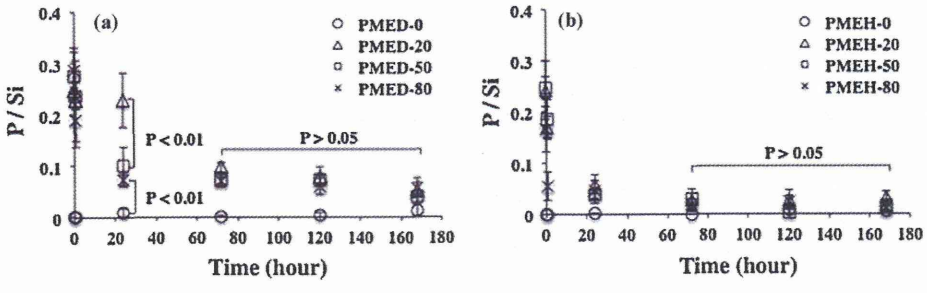

Fig. 7. Time course of the atomic ratio of P/Si on the PDMS surface coated with PMED (a) and PMEH (b) solution.

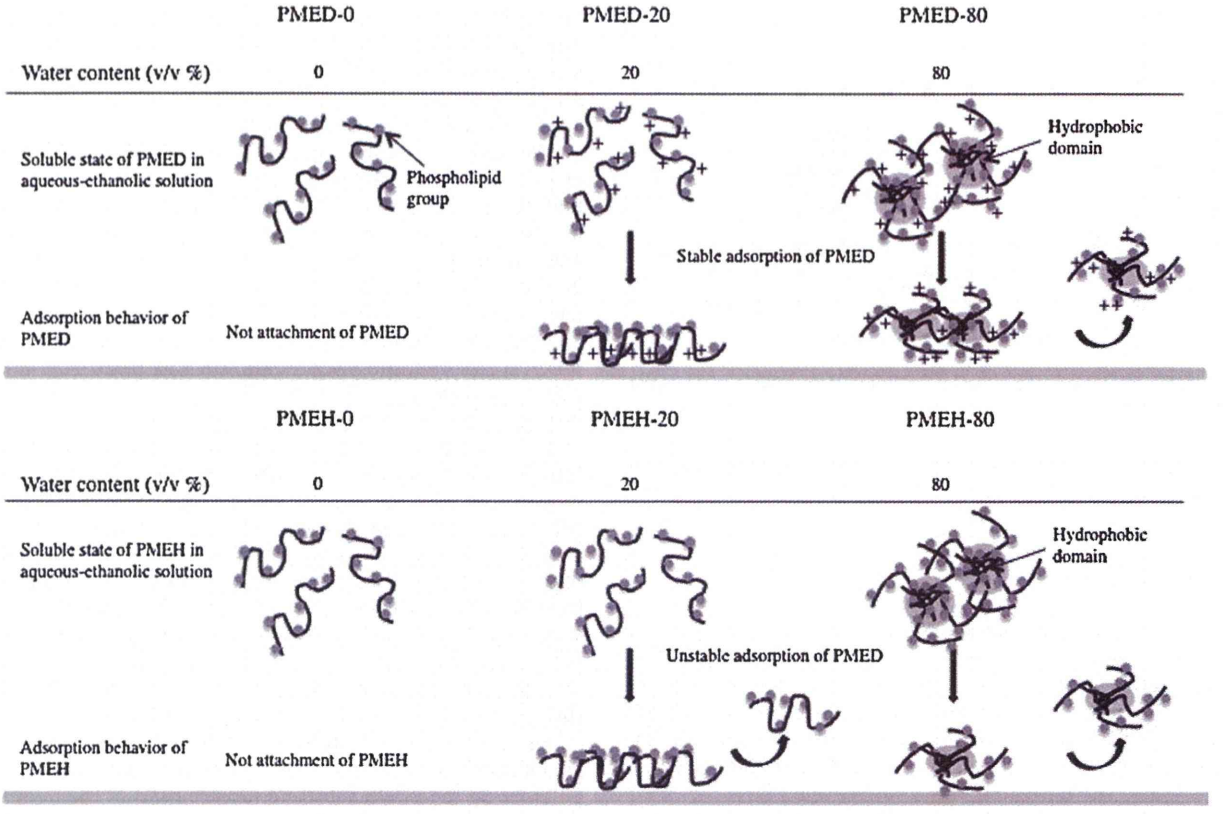

Fig. 8. Schematic illustration of the conformation of PMED and PMEH in aqueous-ethanolic solution and adsorption behavior of PMED and PMEH at PDMS surface.

and the hydrophobic interaction between the polymer chains and the PDMS surface was weakened, PMEH was weakly adsorbed on the PDMS surface. On the other hand, PMED was adsorbed on the PDMS surface primarily via electrostatic forces. Thus, PMED and PMEH may attach to the PDMS surface via either hydrophobic interaction or electrostatic attraction forces. However, both interactions are essential for stable binding between the polymer chains and the PDMS surface. The conformation of a protein is changed after adsorption; the hydrophobic inner surfaces are turned to the outside, and hydrophobic interaction between amino residues and the surface becomes stronger. This is due to the flexible and fragile conformation of proteins. The polymer aggregate is rigid and thermodynamically stable; therefore, the hydrophobic inner region cannot be turned to the outside after adsorption. Thus, the polymer must exist as discrete units in aqueous solution for formation of a stable surface layer, because the hydrophobic interaction between the polymer chains and the surface is weak in the aggregated state.

4. Conclusion

The surface properties of PDMS were readily modified by a simple treatment process using aqueous-ethanolic PMED and PMEH solutions without the need for any pretreatment process. After treatment, the PDMS surface exhibited good water wettability and the dynamic friction coefficient of the surface was decreased by nearly 80% compared with that of the untreated PDMS surface. We demonstrated that the positive charge and hydrophobic moiety were both needed in the polymer for the formation of a stable treatment during treatment of PDMS. Further, we found that the conformation of the polymer in solution influenced the adsorption process. This treatment process is simple and it is possible to apply to various devices made of PDMS after fabrication.

References

[1] M. Chhabra, J.M. Prausnitz, C.J. Radke, Biomaterials 28 (2007) 4331.
[2] M.K. Horne III, K.J. Brokaw, Thromb. Res. 112 (2003) 111.
[3] T.J. Joyce, A. Unsworth, Wear 250 (2001) 199.
[4] J.G. Alauzum, S. Young, R. D'Souza, L. Liu, M.A. Book, H.D. Sheardown, Biomaterials 31 (2010) 3471.
[5] A. Wu, B. Zhao, Z. Dai, J. Qin, B. Lin, Lab Chip 6 (2006) 942.
[6] Y. Yuan, X. Zang, F. Ai, J. Zhou, J. Shen, S. Lin, Polym. Int. 53 (2004) 121.
[7] S. Pintro, P. Alves, C.M. Matos, A.C. Santos, L.R. Rodrigues, J.A. Teixeira, M.H. Gil, Colloids Surf. B: Biointerfaces 81 (2010) 20.
[8] H. Makamba, Y.Y. Hsieh, W.C. Sung, S.H. Chen, Anal. Chem. 77 (2005) 3971.
[9] M. Farrell, S. Beaudoin, Colloids Surf. B: Biointerfaces 81 (2010) 468.
[10] H. Chen, Z. Zhang, Y. Chen, M.A. Brook, H.D. Sheardown, Biomaterials 26 (2005) 2391.
[11] M. Ouyang, C. Yuan, R.J. Muisener, A. Boulares, J.T. Koberstein, Chem. Mater. 12 (2000) 1591.
[12] D. Bodas, C.K. Malek, Microelectr. Eng. 83 (2006) 1277.
[13] M. Morra, E. Occhiello, R. Marola, F. Garbassi, P. Humphrey, D. Johnson, J. Colloid Interface Sci. 137 (1990) 11.
[14] Y. Inoue, T. Nakanishi, K. Ishihara, React. Funct. Polym. 71 (2011) 350.
[15] R. Matsuno, K. Ishihara, NanoToday 6 (2011) 61.
[16] K. Ishihara, N.P. Ziats, B.P. Tierney, N. Nakabayashi, J.M. Anderson, J. Biomed. Mater. Res. 25 (1991) 1397.
[17] K. Ishihara, H. Nomura, T. Mihara, K. Kurita, Y. Iwasaki, N. Nakabayashi, J. Biomed. Mater. Res. 39 (1998) 323.
[18] M. Kyomoto, Y. Iwasaki, T. Moro, T. Konno, F. Miyaji, H. Kawaguchi, Y. Takatori, K. Nakamura, K. Ishihara, Biomaterials 28 (2008) 3121.
[19] M. Kyomoto, T. Moro, K. Saiga, F. Miyaji, H. Kawaguchi, Y. Takatori, K. Nakamura, K. Ishihara, Biomaterials 31 (2010) 658.
[20] S.H. Ye, C.A. Johnson Jr., J.R. Woolley, H. Murata, L.J. Gamble, K. Ishihara, W.R. Wagner, Colloids Surf. B: Biointerfaces 79 (2010) 357.
[21] T. Simizu, T. Goda, N. Minoura, M. Takai, K. Ishihara, Biomaterials 31 (2010) 3274.
[22] T. Moro, Y. Takatori, K. Ishihara, T. Konno, Y. Takigawa, T. Matsushita, U.I. Chung, K. Nakamura, H. Kawaguchi, Nat. Mater. 3 (2004) 829.
[23] T. Moro, H. Kawaguchi, K. Ishihara, M. Kyomoto, T. Karita, H. Ito, K. Nakamura, Y. Takatori, Biomaterials 30 (2009) 2995.